XLVI CILAMCE
VITÓRIA - ES - BRAZIL - 2025
XLVI IBERO-LATIN AMERICAN CONGRESS ON COMPUTATIONAL METHODS IN ENGINEERING

Numerical modeling of skin-core interfacial debonding in composite sandwich beams: a comparative study between continuous and discrete methods.

Eduardo M. Rech[1], Augusto B. de Souza[1], Javier A. Zambrano-Carrillo[2], Ignacio Iturrioz[1], Daniel M. de Leon [1]

[1]*Dept. of Mechanical Engineering, Federal University of Rio-Grande do Sul (UFRGS).*
Rua Sarmento Leite 425, 90050-200, Rio-Grande do Sul, Brazil.
eduardo.miorelli@ufrgs.br, augusto.bisio@ufrgs.br, ignacio.iturrioz@ufrgs.br, daniel.leon@ufrgs.br
[2]*Research Center for Computational Methods (CIMEC), National University of the Littoral (UNL)/National Scientific and Technical Research Council (CONICET).*
Colectora Ruta Nac. 168, S3000, Santa Fe, Argentina.
zambranojavier22@gmail.com

Abstract. Sandwich beams are structures made of different materials with the goal of combining high bending stiffness and low mass. Nevertheless, they are prone to failure modes, especially debonding at the material interfaces. This study focuses on comparing two numerical techniques for modeling the initiation and propagation of such failures: the Cohesive Zone Model (CZM) implemented through Finite Element Methods (FEM), and the Lattice Discrete Element Method (LDEM). The configuration examined comprises fibrous-composite outer skins and a polymeric core bonded by resin-based adhesives, providing valuable guidance on the computational modeling of characteristic failure modes and supporting more informed material and geometry selections when designing sandwich structures. The computational models were reproduced using Altair® HyperMesh and OpitStruct for the FEM implementation and a Fortran code for the LDEM approach. The comparison is carried out through the force versus displacement curve generated by each model, which may serve as a reference for future studies in the field of sandwich beam debonding numerical analysis.

Keywords: sandwich structures, failure mode, debonding, cohesive zone, discrete elements.

1 Introduction

Sandwich structures are composite materials used in various fields of engineering, such as automotive, energy generation, and aerospace, due to their low cost and advantageous high bending stiffness-to-weight ratio. Nevertheless, as stated by Bragagnolo [1], their unique configuration also makes these structures susceptible to several specific failure mechanisms. A particular case is when the damage propagates along the interface between the skin and the core of the sandwich structure, called skin-core debonding. This lack of adhesion, therefore, compromises the integrity of these materials, as debonded regions may lead to crack growth, strength reduction, and ultimately, complete structural failure.

Due to the relevance of this failure mode, various test methods have been developed to characterize the fracture toughness of skin-core debonding in sandwich structures. Bragagnolo [1] describes several, including the double cantilever beam (DCB), cracked sandwich beam (CSB), and single cantilever beam (SCB). These tests differ in how they measure fracture toughness, as different debonding modes may occur – namely Mode I (opening), Mode II (sliding), and Mode III (tearing). Krueger et al. [2] note that critical debonding scenarios are often Mode I dominated, where the skin peels from the core. Weaver [3] states that the SCB test is the most suitable for standardization in this mode due to its simplicity, while Li and Carlsson [4] highlight that tests like the DCB may introduce errors in interfacial toughness measurements.

Due to this characteristic, the SCB test is widely performed, not only at the experimental level but also at the

numerical level, aiming at results validation. This is the case in works such as Schiera and Bisagni [5] and Saeid and Donaldson [6], both of which compared experimental results with numerical data generated using Cohesive Zone Models (CZM) implemented through Finite Element Methods (FEM). More recent studies, however, such as Gasparotto's [7], model sandwich structures in the discrete domain, opting to implement them using Lattice Discrete Element Methods (LDEM). This suggests a promising possibility for using LDEM to model the skin-core debonding process.

In that context, this work intends to expand the use of different numerical models for characterizing the fracture toughness in skin-core debonding. By implementing computational models of FEM-CZM, and DEM, and comparing the three methods with previously obtained experimental results, this paper expands the existing literature on how these techniques may be utilized for this interfacial failure mode of sandwich structures.

2 Methodology

2.1 Experimental test

To numerically model skin-core delamination in sandwich structures, experimental data is needed for comparison. Although a specific standard for Mode I debonding using SCB specimens (ASTM WK90368 [8]) is still under development, ASTM D5528 [9] – originally for DCB Mode I delamination – can be adapted to SCB by adjusting the test setup. Saeid and Donaldson [6] followed this approach in their experimental tests. They used a sandwich beam configuration as shown in Fig. 1, with a thickness of 25.4 mm.

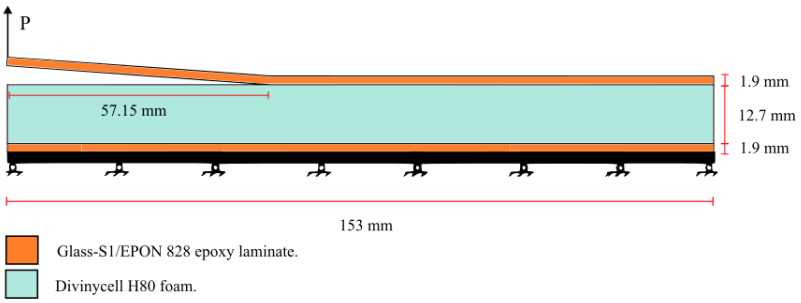


Figure 1 - Schematic of SCB specimen used in the models (based on Saeid and Donaldson [6]).

To compare the numerical simulations with the experimental results of Saeid and Donaldson [6], the geometry will be implemented in the models, as well as the material properties listed in Tab. 1. This includes the interface properties estimated in their study, which are essential for defining the cohesive behavior when implementing CZM.

Table 1 - Model's properties (adapted from Saeid and Donaldson [6]).

Property	Value	Unity
Core's Young's modulus	77.3	MPa
Core's Poisson's Ratio	0.32	-
Skin's Longitudinal Young's modulus	29.29	GPa
Skin's Transversal Young's modulus	10.32	GPa
Skin's In-plane shear modulus	2.79	GPa
Skin's Poisson's ratio	0.18	-
Interface's Cohesive Strength	3.3	MPa
Open Mode Critical Fracture	495.3	J/m^2

2.2 CZM-FEM

The numerical FEM model was set up using Altair HyperMesh 2024.1, and the solver utilized was Altair OptiStruct. For the damage model, CIFHEX and CIFPEN were used as cohesive elements, to represent the cohesive zone. CZM define constitutive laws that relate the forces transmitted across an interface to relative displacement between adjacent surfaces. For the mathematical formulation of the model, consider two material surfaces S^+ and S^-, separated by an interface S, with unit normal vector n . The relative displacement δ between two initially coincident points on S^+ and S^- can be decomposed into normal Δ_n and tangential components Δ_1, Δ_2, using the orthonormal basis $\{n\ , e_1, e_2\}$.

The forces between the solids are expressed as tractions $T = (T_n, T_1, T_2)$, acting oppositely on the S^+ and S^- sides. Since relative displacements are assumed to be small, the formulation is valid under small deformations and rotations. Moreover, interfaces subject to permanent separations require irreversible models, in which fracture energy is dissipated. In such cases, the response depends on the loading history, and the interface cannot heal. A representative example is the scalar damage model proposed by Ortiz and Pandolfi [12] in which degradation is governed by a scalar damage variable $D \in [0,1]$. The energy potential is modified as

$$\Phi(\Delta_n, \Delta_1, \Delta_2, D) = \frac{1}{2} k_0 (1 - D)\lambda^2, \tag{1}$$

where k_0 is the initial stiffness and β is the mixing coefficient

$$\lambda^2 = \Delta_n^2 + \beta^2(\Delta_1^2 + \Delta_2^2). \tag{2}$$

The effective traction magnitude is given by:

$$\tau = \sqrt{(T_n^2 + (T_1^2 + T_2^2)/\beta^2)}, \tag{3}$$

where the traction components are derived from the potential as

$$T_n = k_0(1 - D)\Delta_n,\ T_1 = \beta^2 k_0(1 - D)\Delta_1,\ T_2 = \beta^2 k_0(1 - D)\Delta_2. \tag{4}$$

In the initial phase ($\lambda \leq d_1$), the interface behaves elastically with stiffness k_0. For $\lambda > d_1$, damage D evolves, progressively reducing the interface stiffness until complete failure occurs ($D = 1$), as can be observed in Fig. 3.

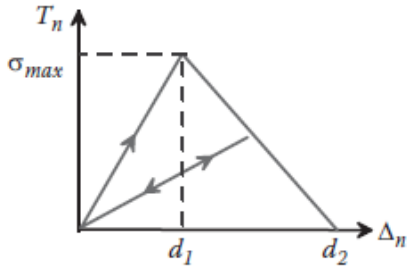


Figure 3 – Bilinear damage evolution (Adapted from Bower [10]).

The evolution of damage can be therefore described by:

$$\frac{dD}{dt} = \begin{cases} 0; & \tau < \frac{(1-D)\left(1+\frac{d_1}{d_2}\right)\sigma_{max}}{1-D+\frac{d_1}{d_2}} \text{ or } d\lambda/dt \ < 0 \text{ or } D = 1 \\ \left((1 - D) + \frac{d_1}{d_2}\right)\frac{1}{\lambda}\frac{d\lambda}{dt}; & \text{Otherwise} \end{cases}, \tag{5}$$

and the total fracture energy is determined by the peak traction σ_{max} and by the displacement δ:

$$\phi_0 = \frac{1}{2}\sigma_{max}(\delta_1 + \delta_2),\ \sigma_{max} = k_0\delta_1 \tag{6}$$

2.3 LDEM

The Lattice Discrete Element Method (LDEM) is a numerical technique, which was implemented using a Fortran code and visualized through Ansys® APDL, based on the discretization of a continuum domain using a regular network of uniaxial elements connecting nodal points. Each node concentrates mass and has three translational degrees of freedom along orthogonal directions. According to Kosteski et al [11] these elements interact solely through axial forces, enabling the natural simulation of damage initiation, propagation, and fragmentation in quasi-brittle materials. The LDEM mesh consists of cubic cells containing 9 nodes connected by 20 longitudinal and diagonal bars. According to Nayfeh and Hefzy [12], this configuration reproduces the behavior of an orthotropic elastic continuum, with exact equivalence to isotropic behavior when the Poisson ratio is ν = 0.25. The cross-sectional areas A_n and A_d of the longitudinal and diagonal bars, respectively, are defined as

$$A_n = \phi L^2 \text{ and } A_d = \frac{2}{\sqrt{3}\delta}A_n, \tag{7}$$

in such way that *L* is the length of the basic cubic module,

$$\phi = \frac{9+8\delta}{18+24\delta} \text{ and } \delta = \frac{9\nu}{4-8\nu}. \tag{8}$$

The motion equation for each node is derived from Newton's second law:

$$\tilde{M}\ddot{x}(t) + \tilde{C}\dot{x}(t) + \tilde{F}(t) - \tilde{P}(t) = 0, \tag{9}$$

where $\tilde{M}$ is the diagonal mass matrix, $\tilde{F}(t)$ are the internal nodal forces, $\tilde{P}(t)$ are the external applied forces and $\tilde{C}$ is the damping matrix, defined as:

$$\tilde{C} = 2\pi\xi f_p, \tag{10}$$

with ξ being the damping ratio and f_p the peak frequency of the energy spectrum. The system is solved in the time domain using an explicit finite difference scheme, which avoids the need for rotation tracking or coordinate transformations, even for large displacements.

Each bar follows a bilinear uniaxial constitutive law with a softening branch under tension, based on Hillerborg's proposal for quasi-brittle materials. The material behaves elastically up to the peak strain ε_p , after which a descending branch leads to fracture at the critical strain ε_r. The area under the stress-strain curve corresponds to the fracture energy G_f. The critical strain is given by:

$$\varepsilon_r = \varepsilon_p d_{eq}\left(\frac{2A_i^{'}}{A_i L_i}\right), \tag{11}$$

where d_{eq} is the material's characteristic length, $A_i^{'}$ is the equivalent fracture area of bar i and A_i and L_i are the cross-sectional area and length of the bar, respectively. A bar is considered fractured (i.e., it loses its load-carrying capacity) when $\varepsilon \geq \varepsilon_r$. Under compression, the behavior is assumed to remain linearly elastic, and failure is induced indirectly by transverse tension. The damage is modeled progressively, allowing for both distributed and localized deformation patterns up to final rupture. To reflect the heterogeneous nature of quasi-brittle materials, the LDEM incorporates random material properties.

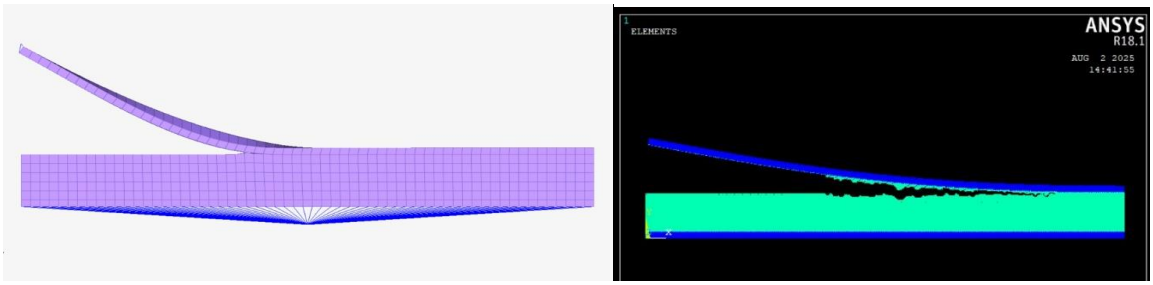
Moreover, the peak strain ε_p is computed as

$$\varepsilon_p = \sqrt{\frac{\mu_{G_f}}{E d_{eq}}}, \tag{12}$$

where the fracture energy Gf is modeled as a 3D random field following a Weibull distribution, characterized by a mean value μGf coefficient of variation CV and spatial correlation length L_c. Interpolation between discrete poles in the mesh domain provides the spatial distribution of Gf values assigned to each bar, preserving the desired correlation structure.

3 Results

The implementation of the skin-core debonding problem using both FEM-CZM and LDEM was successfully achieved in the respective numerical setups, demonstrating that the modeling approach is feasible within each framework, as can be seen in Fig. 4. It is interesting noticing, however, that the CZM-FEM model was not able to capture the debonding progression, while the LDEM model provided results similar to the experimental observations, highlighting an advantage in applying this type of model to debonding problems which require crack propagation analysis.



a) b)

Figures 4 – Numerical models of the SCB test: a) CZM-FEM model; b) LDEM model.

Aiming for a more detailed distinction between these models, the force versus displacement curve was obtained for the experimental (extracted using WebPlotDigitizer) and for the numerical CZM-FEM. By comparing them, in Fig. 5, it is possible to observe similar behavior in the curves, such as the maximum force values being 58.25 N and 59.05 N respectively. The peak force, although similar in magnitude to the experimental results, was achieved at higher opening mode displacements than those observed experimentally. Furthermore, it is worth mentioning that the model did not properly simulate the full debonding and was only able to capture the initiation stage, showing conversion problems as the model reaches the crack propagation through the core.

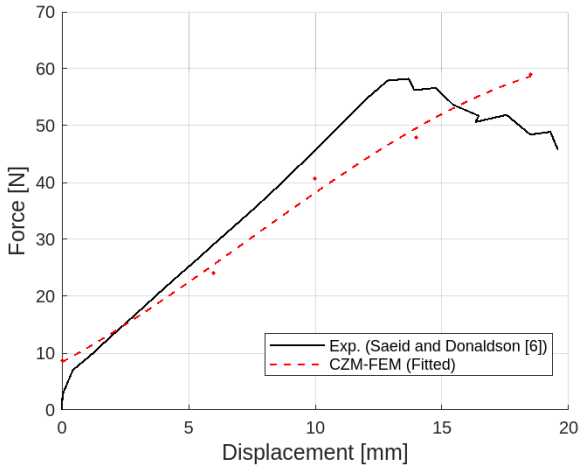


Figure 5 – Force versus displacement comparing the experimental results with the CZM-FEM modeling.

In the case of the LDEM simulation, despite being possible to simulate the crack propagation, the results also exhibited a high level of variation and noise throughout the force versus displacement response, as can be seen in Fig. 6. This behavior is likely associated with the discrete nature of the method and the sensitivity of the model to parameters such as particle size, contact stiffness, and damping.

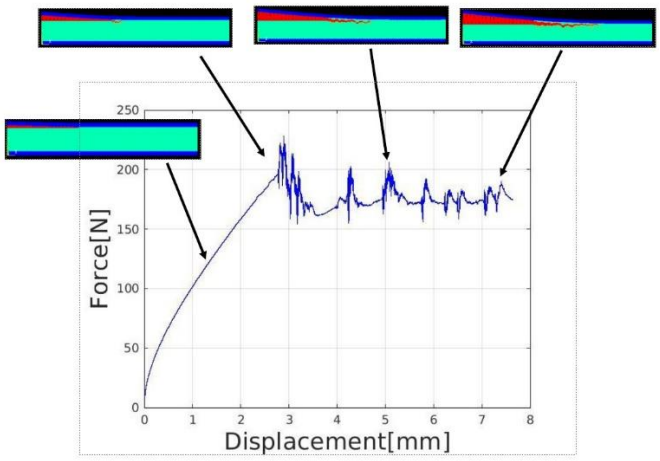


Figure 6 – Force versus displacement curve throughout the debonding stages obtained using the LDEM model.

This indicates the need for a more thorough calibration of these parameters to achieve a closer match with the experimental curve, which will be addressed in future work. However, from a physical standpoint, in terms of the deformation response and crack propagation, a satisfactory capture is observed. This is also evidenced in the energy curves of Fig. 7, where the behavior of the elastic, dissipative, and kinetic energies is presented.

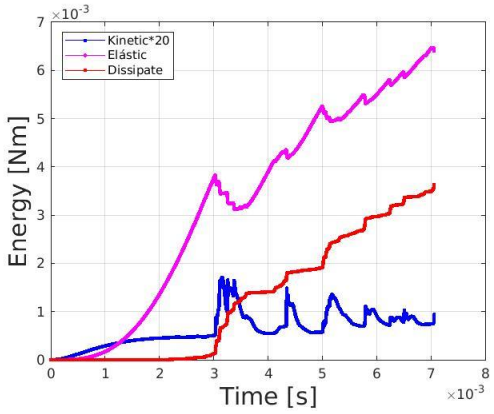


Figure 7 – Energy curves for skin–core debonding generated using the LDEM model.

4 Conclusions

The implementation and comparison of different numerical methods for modeling skin-core debonding in sandwich structures proved to be not only feasible, but also essential for expanding the existing literature and serve as valuable references for future reviews and methodological developments in the field. The results highlight the sensitivity of all approaches to modeling parameters, with particular emphasis on the LDEM, which demonstrated a strong dependency on calibration and exhibited significant variability. Nevertheless, despite the noise-related discrepancies, the LDEM was able to simulate the complete crack propagation, reinforcing its potential for accurately capturing debonding behavior.

On the other hand, the FEM-CZM approach stands out for its relative ease of implementation and lower computational cost, making it an accessible option for initial investigations. However, it may also present significant deviations when compared to experimental results, particularly in capturing the full progression of the debonding process. This reinforces the importance of careful validation when using FEM-based models for skin-core debonding analysis in sandwich structures, and the need to use other methods to model the interfacial crack, such as the extended finite element method (XFEM).

Therefore, the comparison between the models showed that for more detailed analyses, the LDEM model proved to be more representative of the actual debonding behavior, particularly in capturing the full crack propagation. However, this advantage comes at the cost of increased calibration effort, due to the model's high sensitivity to input parameters. On the other hand, for quicker assessments, the CZM-FEM model provided a good representation of the elastic region preceding crack initiation, allowing for a relatively easy estimation of the peak load. This makes it a practical choice for preliminary evaluations or situations where computational efficiency is a priority.

In conclusion, this work contributes to building a foundation for more robust and comparative modeling frameworks, supporting both academic research and engineering applications. As next steps, efforts will focus on the proper calibration of the DEM model to reduce noise and improve its ability to represent the debonding process more accurately. In addition, the implementation of alternative approaches, such as the Phase-Field Method, will be explored, as it may offer a more consistent description of crack propagation in interface debonding failure. These developments aim to enhance the reliability and completeness of numerical modeling for skin-core debonding in sandwich structures.

Authorship statement: The authors hereby confirm that they are the sole liable persons responsible for the authorship of this work, and that all material that has been herein included as part of the present paper is either the property (and authorship) of the authors, or has the permission of the owners to be included here.

References

[1] G. Bragagnolo. Experimental and Numerical Investigation of Debonding in Automotive Composite Structures. EngD thesis, University of Surrey, 2019.
[2] R. Krueger et al., "Characterizing Face Sheet/Core Disbonding Using the Single Cantilever Beam Test: Results from an International Round Robin", NASA/TM–20240001178, 2024.
[3] C. Weaver. Evaluation of Mode I Fracture Mechanics Test Methods for Sandwich Composites. M.Sc Thesis, University of Utah, 2009.
[4] X. Li and L.A. Carlsson. "Elastic foundation analysis of tilted sandwich debond (TSD) specimen." *J Sandw Struct Mater*, vol. 2, pp. 3–32, 2000.
[5] M. Schiera and C. Bisagni. "Numerical Modelling of Interface Delamination in Sandwich Composite Structures". *14th International Conference on Sandwich Structures (ICSS-14).*
[6] A. A. Saeid and S. L Donaldson. "Experimental and finite element evaluations of debonding in composite sandwich structure with core thickness variations". *Advances in Mechanical Engineering*, vol. 8, n. 9, pp. 1–18, 2016.
[7] B. G. Gasparotto. Applied Structural Stability in the Context of LDEM. M.Sc Thesis, Federal University of Rio-Grande do Sul, 2017 (in Portuguese).
[8] ASTM Subcommittee D30.09, "ASTM WK90368, New Test Method for Mode I Dominant Facesheet-to-Core Fracture Toughness of Sandwich Constructions", under development within ASTM Committee.
[9] ASTM International, "ASTM D5528, Standard test method for mode I interlaminar fracture toughness of unidirectional fiber reinforced polymer matrix composites", ASTM International, 2007.
[10] A.F. Bower. *Applied Mechanics of Solid.* Taylor and Francis Group, 2010.
[11] L. E. Kosteski et al. "A study by the lattice discrete element method for exploring the fractal nature of scale effects." *Scientific Reports*, vol. 12, n. 16744, 2022.
[12] A. H. Nayfeh and M. S. Hefzy. "Continuum modeling of three-dimensional truss-like space structures." *AIAA J*, vol. 16, n. 8, 1978.